

PROCESS INDUCED TRANSVERSE SHEAR STRESSES IN THICK UNIDIRECTIONAL PULTRUDED PROFILES

Ismet Baran¹, Remko Akkerman²

¹Chair of Production Technology, Faculty of Engineering Technology, University of Twente, 7500AE, Enschede, The Netherlands

Email: i.baran@utwente.nl, Web Page: <https://www.utwente.nl/ctw/pt/>

²Chair of Production Technology, Faculty of Engineering Technology, University of Twente, 7500AE, Enschede, The Netherlands

Email: i.baran@utwente.nl, Web Page: <https://www.utwente.nl/ctw/pt/>

Keywords: Pultrusion, Transient stresses, Transverse shear, Thick composite, Process modelling

Abstract

The residual stresses in the transverse to the fiber direction might be critical for unidirectional composites since their transverse shear strength is relatively low. Transverse shear behavior therefore needs to be analyzed carefully for thick pultruded profiles which have been increasingly used in structural load bearing applications. This is a necessary task to avoid potential crack formation during the process and to minimize the process induced damage level. In the present work the process induced residual stresses are predicted for a 100×100 mm unidirectional pultruded square profile made of glass/polyester. A thermochemical model is coupled with a mechanical model using the finite element method. The temperature and degree of cure distributions are calculated for three different preheating temperature defined at the pultrusion die inlet, namely $T_{inlet} = 20\text{ °C}$, 40 °C and 60 °C . Mechanical constraints are formed due to the through thickness cure gradients and elastic modulus variation. The nonuniform internal constraints yield in an internal shear deformation. The transverse shear stresses are found to be more critical than the transverse normal stresses in tension.

1. Introduction

Pultruded products have increasingly been used in transportation and wind energy industries as load carrying pre-fabricated components. One example is the wind turbine blade root reinforcement which is a relatively thick fiber reinforced polymer composite manufactured by pultrusion [1]. In order to have a better structural reliability of the composite structures consisting of pultruded parts during the service life, the mechanical performance of the pultruded parts need to be understood well. Therefore, it is necessary to characterize the pultrusion process to manufacture high quality pultruded profiles with minimum defects or improved mechanical performance. Although pultrusion process is a continuous and automated process, the involved multi-physics make the process difficult to control. A schematic view of the thermosetting pultrusion process is depicted in Fig 1. The thermosetting resin is gradually cured in the heated die in which the status of the resin changes from liquid to rubbery and finally to solid. The cured profile is pulled by a pulling mechanism and cut into desired length by a saw.

One of the main challenges in pultrusion process is the process induced residual stresses since they may cause manufacturing induced defects in the product such as premature cracking, delamination and shape distortions [2]. The main mechanisms generating the process induced residual stresses for thermosetting

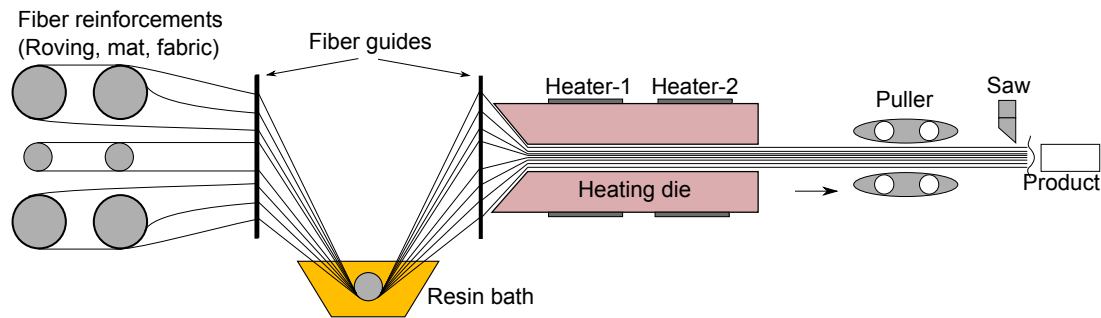


Figure 1. Schematic view of a thermosetting pultrusion process with a resin bath impregnation system.

composites can be listed as [3, 4] (i) the tool-part interaction, (ii) the chemical shrinkage during polymerization, (iv) the through-thickness degree of cure, and (v) the fiber volume fraction gradients. The degree of cure gradients through the thickness due to temperature lags and chemical exotherms can be important in thick composite parts, and may cause additional residual stresses [5]. The residual stresses in the transverse to the fiber direction even might be more critical for unidirectional (UD) composites since their transverse shear strength is relatively low. The transverse shear strength of a UD glass/epoxy composite was found to be around 7 MPa using short beam shear tests in [6].

The residual stresses for pultrusion processes have been predicted in several studies in literature. A state-of-the-art numerical modelling framework was developed by Baran et al. [7] to predict the residual stresses and shape distortions in pultrusion processes. A finite element model was employed in which a three dimensional (3D) thermo-chemical model was coupled with a 2D quasi-static mechanical model. A square UD glass epoxy square profile (25.4×25.4 mm) was analyzed using the proposed model. A UD graphite/epoxy rod was studied in [8] in which the diameter of the rod was 9.5 mm. The stress levels were found to be relatively small (< 1 MPa) due to the quite uniform temperature and curing evolutions in the part. A thermo-chemical-mechanical analysis of the pultrusion process was presented in [9]. A process simulation was performed for an industrially pultruded rectangular hollow profile (64×27 mm) with a thickness of 3 mm containing both UD roving and continuous filament mat (CFM) layers. A numerical simulation tool was developed to calculate the process induced stresses and dimensional variations in an industrially pultruded L-shaped profile in [10]. The cross sectional dimensions of the part were 50×50 mm with a thickness of 5 mm and it contained glass/polyester based UD roving and CFM layers. In [11], process simulations for the pultrusion of a C-section profile (400×120 mm) with a thickness of 18 mm were carried out. Profile reinforcement was built up of UD glass rovings oriented in a longitudinal direction with the outer layer of fiberglass fabric. A warpage behaviour was investigated using the proposed model [11].

As compared with the aforementioned literature on pultrusion process, much thicker UD solid pultruded square profile (100×100 mm) is studied in this work which has not been considered up to now. The model proposed in [7] is implemented to predict the temperature and degree of cure evolution during the pultrusion process. The process induced residual stresses are predicted and the effect of preheating of inlet temperature on the stress evolution are investigated. The formation of the transverse shear stresses are explained and compared with the transverse normal stresses.

2. Numerical Implementation

The finite element model developed in [7] is employed. A schematic view of the sequential coupling of the thermo-chemical model and the mechanical model is depicted in Fig. 2. In the thermo-chemical model, a 3D heat transfer equation is solved using the general purpose finite element software package

ABAQUS for the composite part as well as for the die. The advective term due to the pulling speed of the composite part and the internal heat generation due to exothermic reaction are included in the heat transfer model (Eq. 1).

$$(\rho C_p) \left(u \frac{\partial T}{\partial x_1} \right) = k_{x_1} \frac{\partial^2 T}{\partial x_1^2} + k_{x_2} \frac{\partial^2 T}{\partial x_2^2} + k_{x_3} \frac{\partial^2 T}{\partial x_3^2} + q \quad (1)$$

where T is the temperature, u is the pulling speed, ρ is the density, C_p is the specific heat and k_{x_1} , k_{x_2} and k_{x_3} are the thermal conductivities along x_1 -, x_2 - and x_3 -directions, respectively. Here, x_1 is the pulling or longitudinal direction; x_2 and x_3 are the transverse directions for the UD pultruded part. The internal heat generation is defined as a function of the thermosetting resin density, total heat of reaction during exothermic curing reaction and the curing rate which is expressed in Eq. 2 [7, 12].

$$q = (1 - V_f) \rho_r H_{tr} R_r(\alpha, T) \quad (2)$$

where H_{tr} is the total heat of reaction for the resin, ρ_r is the resin density, V_f is the fiber volume fraction, α is the degree of cure, and $R_r(\alpha, T)$ is the reaction of cure which can also be defined as the rate of α , i.e. $d\alpha/dt$. The expression for the cure kinetics is given as:

$$R_r(\alpha, T) = \frac{d\alpha}{dt} = A_0 \exp\left(\frac{-E_a}{RT}\right) \alpha^m (1 - \alpha)^n \quad (3)$$

where A_0 is the pre-exponential constant, E_a is the activation energy, R is the universal gas constant, m and n are the order of reaction (kinetic exponents).

In the 2D quasi-static mechanical model, the elastic modulus of the resin is modelled using the cure hardening instantaneous linear elastic (CHILE) approach proposed by Johnston [13]. The effective mechanical properties of the UD layer are calculated using the self consistent field micromechanics (SCFM) approach which is a well known and documented technique in the literature [5]. An incremental linear elastic approach is implemented utilizing the user defined subroutines in ABAQUS to calculate the displacements and stresses. The total incremental strain ($\dot{\varepsilon}^{tot}$), which is composed of the incremental mechanical strain ($\dot{\varepsilon}^{mech}$), thermal strain ($\dot{\varepsilon}^{th}$) and chemical strain ($\dot{\varepsilon}^{ch}$), is given in Eq. 4. Here, the incremental process induced strain ($\dot{\varepsilon}^{pr}$) is defined as the summation of $\dot{\varepsilon}^{th}$ and $\dot{\varepsilon}^{ch}$ as also done in e.g. [5, 13]. The incremental stress tensor ($\dot{\sigma}_{ij}$) is calculated using the material Jacobian matrix (\mathbf{J}) based on the incremental mechanical strain tensor ($\dot{\varepsilon}^{mech}$) (Eq. 5).

$$\begin{aligned} \dot{\varepsilon}_{ij}^{tot} &= \dot{\varepsilon}_{ij}^{mech} + \dot{\varepsilon}_{ij}^{th} + \dot{\varepsilon}_{ij}^{ch} \\ \dot{\varepsilon}_{ij}^{pr} &= \dot{\varepsilon}_{ij}^{th} + \dot{\varepsilon}_{ij}^{ch} \\ \dot{\varepsilon}_{ij}^{mech} &= \dot{\varepsilon}_{ij}^{tot} - \dot{\varepsilon}_{ij}^{pr} \end{aligned} \quad (4)$$

$$\dot{\sigma}_{ij} = \mathbf{J} \dot{\varepsilon}_{ij}^{mech} \quad (5)$$

The stress and strain tensors are updated at the end of the each time increment as in Eq. 6 and Eq. 7, respectively.

$$\sigma_{ij}^{n+1} = \sigma_{ij}^n + \dot{\sigma}_{ij}^n \quad (6)$$

$$\varepsilon_{ij}^{n+1} = \varepsilon_{ij}^n + \dot{\varepsilon}_{ij}^n \quad (7)$$

Further details of the numerical implementation can be found in [2, 7].

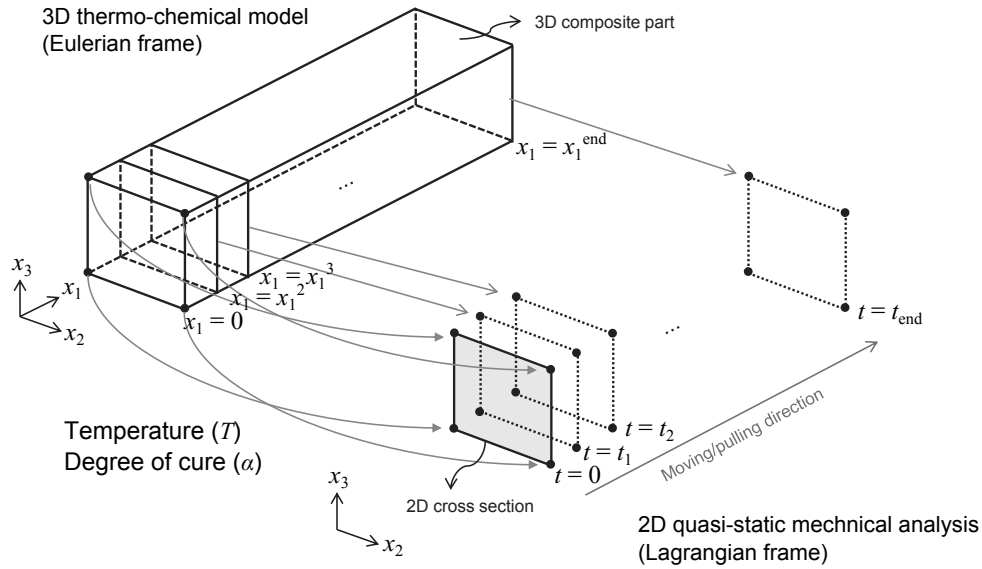


Figure 2. Representation of the sequentially coupled 3D thermo-chemical model with a 2D quasi-static mechanical model for pultrusion processes [7].

3. Pultrusion Model

The pultrusion model developed in [10] for an industrial glass/polyester composite is implemented in the present work. Only a quarter of the pultrusion domain, seen in Fig. 3, is modeled due to symmetry. A steel die is used for die block. The pulling speed is set to 100 mm/min which is much lower than the speed used in [10] (600mm/min). This is due to the fact that the thickness of the composite in this work is 20 times larger than the thickness of the composite in [10] (5 mm). The fiber orientation is defined along the pulling direction (i.e., x_1 -direction). Material models for the composite are also taken from [10]. Two heating zones having prescribed set temperatures 110 °C and 140 °C are defined. At the inlet of the pultrusion die, the temperature of all the nodes attached to the composite are set to a inlet temperature (T_{inlet}) as a prescribed temperature boundary condition. T_{inlet} mimics the preheating temperature of the resin and fiber before entering the pultrusion die. Perfect thermal contact is assumed at the die-part interface. At the symmetry surfaces adiabatic boundaries are defined in which no heat flow is allowed across the boundaries. The remaining exterior surfaces of the die are exposed to ambient temperature with a convective heat transfer coefficient of 10 W/(m²-K) except for the surfaces located at the heating regions. Similarly, at the post-die region, convective boundaries are defined for the exterior surfaces of the square profile.

In the 2D mechanical analysis of the pultrusion process, the cross section of the composite is moved through the pulling direction during the process (Lagrangian frame) meanwhile tracking the corresponding temperature and degree of cure profiles already calculated in the 3D thermo-chemical analysis (Eulerian frame) as described in Fig. 2. Since the cross sectional dimensions are much smaller than the total length of the pultrusion line in the pulling direction (x_1 -direction, a plane strain assumption is made for the residual stress analysis in which no strain component is taken into account in the pulling direction (the out of plane strain is assumed to be zero in Eq. 5).

4. Results and Discussions

The temperature and degree of cure distributions are calculated from the point at which part enters the pultrusion die till the part cools down to ambient temperature (20 °C). A parametric study is carried out

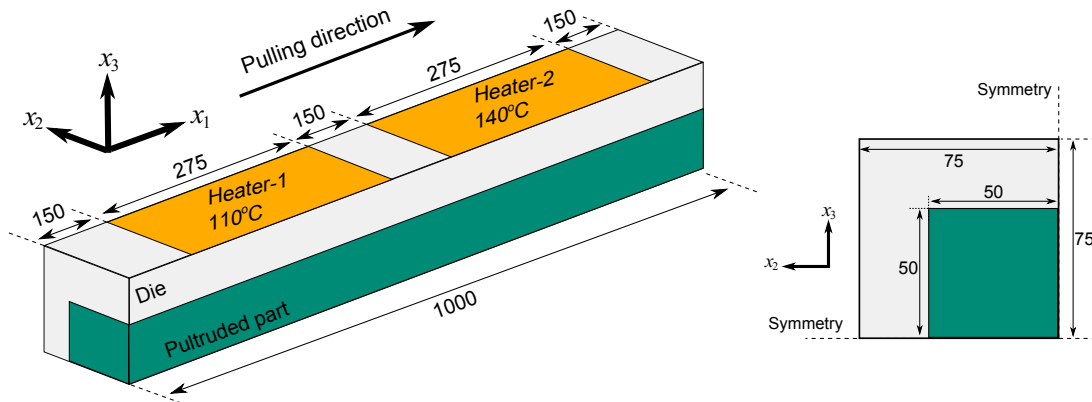


Figure 3. Schematic view of the quarter pultrusion domain for a UD glass/polyester profile. All dimensions are in mm and the fiber orientation is in x_1 -direction.

using different preheating temperature (T_{inlet}). The degree of cure distributions at the die exit (i.e., at $x_1 = 1$ m) and when the part cools down to room temperature are depicted in Fig. 4 and Fig. 5, respectively for different T_{inlet} values namely 20 °C, 40 °C and 60 °C. It is seen from Fig. 4 that with higher inlet or preheating temperature larger portion of the cross section is cured with a degree of cure value above 0.85. The inner region is not cured at the die exit. However, the curing of the inner portion takes place at post die since the temperature of the outer region is still high to initiate the exothermic reaction of the inner region. When the part cools down to room temperature, it is seen from Fig. 5 that the degree of cure is almost 1 (fully cured) for higher T_{inlet} values (40 °C and 60 °C), on the other hand some portion of the cross section is not fully cured for the case with $T_{inlet} = 20$ °C having a degree of cure value around 0.85. The reason for this is that the temperature at the post die is not fully sufficient for the complete exothermic reaction with $T_{inlet} = 20$ °C.

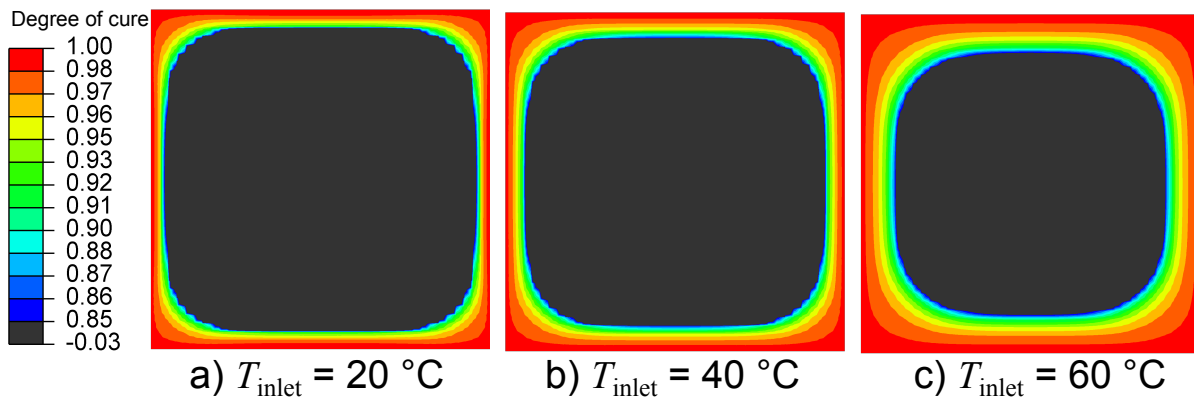


Figure 4. Degree of cure distribution at the pultrusion die exit for different T_{inlet} values.

The temperature evolution at the center and top (outer surface) of the part is depicted in Fig. 6. The dashed circles in Fig. 6 indicates the point at which the temperature of the center becomes larger than the temperature of the top (outer surface) due to the curing process. It is seen that curing takes place at later stages in time (and hence in position) for the case with $T_{inlet} = 20$ °C. More specifically, curing begins approximately at 2 m, 3 m and 4 m for $T_{inlet} = 60$ °C, 40 °C and 20 °C, respectively.

The predicted transverse normal stress (σ_{22}) and transverse shear stress (τ_{23}) distribution when the part cools down to room temperature are shown in Fig. 7 and Fig. 8, respectively. It is seen that τ_{23} becomes more critical than σ_{22} for $T_{inlet} = 20$ °C. A value of approximately 12.4 MPa is found for τ_{23} which is

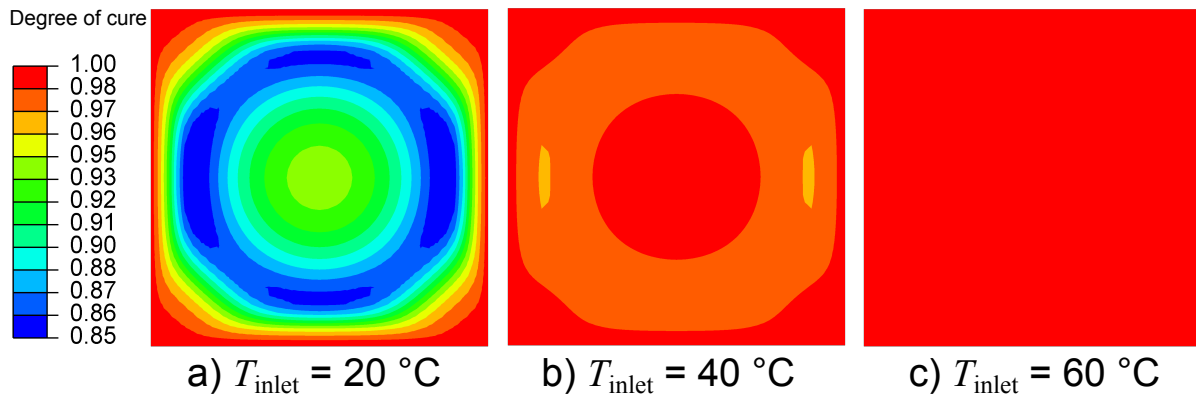


Figure 5. Degree of cure distribution when the pultruded part cooled down to room temperature (20 °C) for different T_{inlet} values.

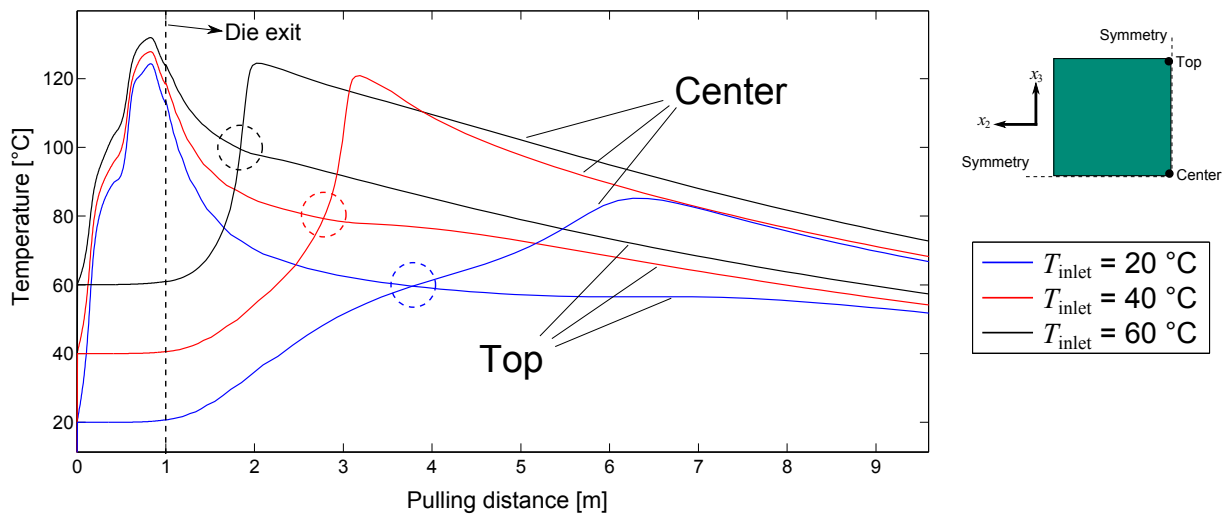


Figure 6. Temperature evolution at at the center and top (outer surface) as a function of pulling distance. Note that temperature goes down to room temperature in the numerical simulations, however for the sake of visualization it is not plotted.

larger than $\sigma_{22} = 8.6$ MPa. This indicates that transverse stresses are more pronounced when the cure and elastic modulus gradients through the thickness are higher. It is seen that higher stress values are obtained for the case with $T_{inlet} = 20$ °C. The curing lag between the center and top as seen in Fig. 6 causes internal mechanical constraints to the inner region which cures later as compared with the outer region of the pultruded part. During curing, the outer region shrinks towards symmetry surfaces while no deformation takes place at the inner region. When the outer region cures, the elastic modulus increases as a function of the glass transition temperature which is defined in the CHILE model for the resin modulus [2]. The degree of mechanical constraint exerted by the cured and solidified outer region is hence influenced by the temperature of the outer surface since higher temperatures yield in lower elastic modulus at the glass state. In other words, harder mechanical constraint takes place for lower temperature of the cured region and softer constraint is the case for higher temperature at glass state. As a results, higher stresses prevail for $T_{inlet} = 20$ °C since the temperature of the outer region is approximately 60 °C when the inner region (center) starts curing (see dashed circle in Fig. 6). The predicted stress levels decrease with an increase in T_{inlet} since more uniform curing is accommodated in the part.

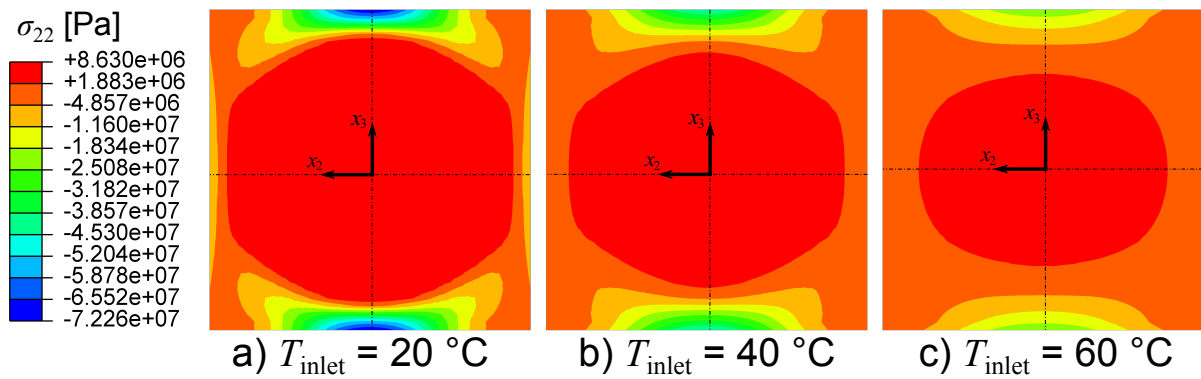


Figure 7. Transverse normal stress distribution (σ_{22}) at the cross section for different T_{inlet} values when the pultruded part cooled down to room temperature (25 °C). Note that the maximum σ_{22} value is 8.6 MPa, 7.5 MPa and 6.4 MPa for $T_{inlet} = 20\text{ }^{\circ}\text{C}$, 40 °C and 60 °C, respectively.

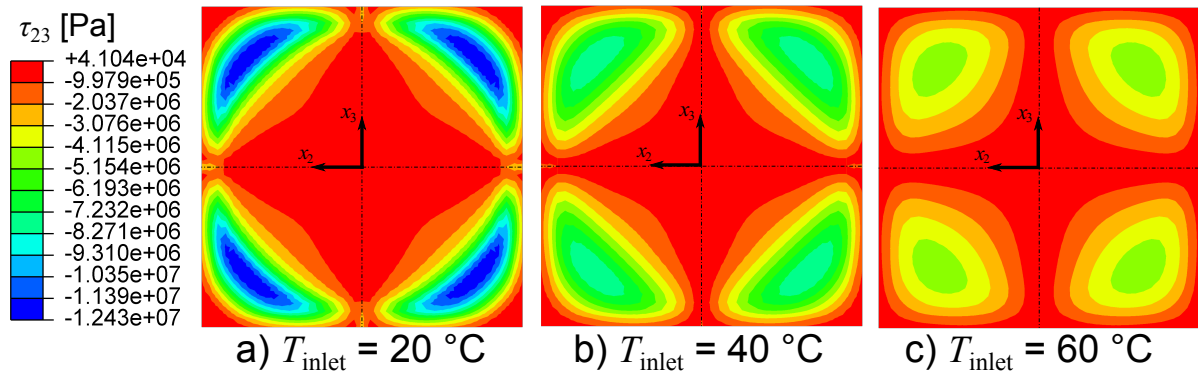


Figure 8. Transverse shear stress distribution (τ_{23}) at the cross section for different T_{inlet} values when the pultruded part cooled down to room temperature (25 °C).

5. Conclusion

In this paper, the process induced residual stresses were predicted for the pultrusion of a UD glass/polyester square profile (100×100 mm). A thermo-chemical model was coupled with a mechanical model. The temperature and degree of cure distributions were calculated for three different inlet temperature of the composite at the pultrusion die inlet, namely $T_{inlet} = 20\text{ }^{\circ}\text{C}$, 40 °C and 60 °C. Relatively large cure gradients were found to exist in all cases which yielded in internal mechanical constraint in the part during processing. Once the inner region starts curing, the outer region which is already cured and solidified acts as a mechanical constraint. The degree of constraint is dependent on the stiffness of the cured region. Higher temperature provides a less stiff constraint at the glassy state. Therefore, lower stress level is obtained for $T_{inlet} = 40\text{ }^{\circ}\text{C}$ and 60 °C, whereas higher residual stress level was found for the case without heating the resin/fiber before entering the die (i.e. $T_{inlet} = 20\text{ }^{\circ}\text{C}$). The transverse shear stresses ($\tau_{23} = 12.4\text{ MPa}$) were found to be more critical than the transverse normal stresses ($\sigma_{22} = 8.6\text{ MPa}$) considering the strength values for transverse shear and normal. The transverse shear stress magnitude was found to decrease with a higher preheating (inlet) temperature. Taking relatively low transverse shear strength of UD composites (3-7 MPa [6]) into account, the transverse shear stresses need to be carefully analyzed for thick UD pultruded profiles since there may be cracking in the manufactured part.

References

- [1] I. Baran. *Pultrusion: State-of-the-art Process Models*. Smithers Rapra, Shropshire, UK, 2015.
- [2] I. Baran. *Modelling the pultrusion process of off shore wind turbine blades*. PhD thesis, Technical University of Denmark, 2014.
- [3] M.R. Wisnom, M. Gigliotti, N. Ersoy, M. Campbell, and K.D. Potter. Mechanisms generating residual stresses and distortion during manufacture of polymer-matrix composite structures. *Composites Part A*, 37:522–529, 2006.
- [4] I. Baran, K. Cinar, N. Ersoy, R. Akkerman, and J.H. Hattel. A review on the mechanical modeling of composite manufacturing processes. *Archives of Computational Methods in Engineering*, pages 1–31, 2016.
- [5] T.A. Bogetti and J.W. Gillespie. Process-induced stress and deformation in thick-section thermoset composite laminates. *Journal of Composite Materials*, 26:626–660, 1992.
- [6] E. Sideridis and G.A. Papadopoulos. Short-beam and three-point-bending tests for the study of shear and flexural properties in unidirectional-fiber-reinforced epoxy composites. *Journal of Applied Polymer Science*, 93.(1):63–74, 2004.
- [7] I. Baran, C.C. Tutum, M.W. Nielsen, and J.H. Hattel. Process induced residual stresses and distortions in pultrusion. *Composites Part B: Engineering*, 51:148–161, 2013.
- [8] P. Carlone, I. Baran, J.H. Hattel, and G.S. Palazzo. Computational approaches for modelling the multi- physics in pultrusion process. *Advances in Mechanical Engineering*, Article ID 301875:1–14, 2013.
- [9] I. Baran, J. H. Hattel, and R. Akkerman. Investigation of process induced warpage for pultrusion of a rectangular hollow profile. *Composites Part B: Engineering*, 68:365–374, 2015.
- [10] I. Baran, R. Akkerman, and J. H. Hattel. Modelling the pultrusion process of an industrial l-shaped composite profile. *Composite Structures*, 118:37–48, 2014.
- [11] A.A. Safonov and A.Yu. Konstantinov. Numerical evaluation of residual manufacturing deformations in complex pultruded composite profiles. In *20th International Conference on Composite Materials*, Copenhagen, Denmark, 19-24th July 2015.
- [12] I. Baran. Pultrusion processes for composite manufacture. In *P. Boisse editor. Advances in Composites Manufacturing and Process Design*, Woodhead Publishing, Cambridge, UK, 2015.
- [13] A. Johnston. *An integrated model of the development of process-induced deformation in autoclave processing of composite structures*. PhD thesis, University of British Columbia, Vancouver, Canada, 1997.